Optimizing Energy Use and Thermal Comfort with Model Predictive Control for Hydronic Floors: An Experimental Case Study

Grace Dhaliwal, Burak Gunay, Ian Beausoleil-Morrison
Carleton University, Ottawa, Canada

Abstract

Despite the popularity of model predictive controllers (MPCs) in building automation, experimental studies and investigations of their application to residential buildings are limited. Existing studies highlight MPCs' potential in buildings with high glazing and hydronic floor conditioning, such as the Urbandale Center for Home Energy Research (CHEeR), an experimental facility in Ottawa, Canada that mimics a single detached house. This paper presents the development and initial results of a long-term MPC implementation study at CHEeR during the heating season. The MPC optimizes hydronic floor operation to maintain thermal comfort and minimize energy use. This work provides a novel approach to disturbance forecasting and parameter estimation. Disturbances are forecasted using a clustering algorithm, followed by rule extraction with a decision tree, and techniques previously used for fault impact analysis are used for parameter estimation. Compared to a rule-based controller (RBC), the MPC used 15% less energy overall, and mitigated overheating. However, its performance was slightly degraded in maintaining temperatures above the lower comfort threshold.

Introduction

In 2019, residential energy use accounted for 15% of Canada's total energy consumption, with 65% allocated to space heating and cooling (Natural Resources Canada, 2019, nd). Significant energy savings can therefore be realized by improving HVAC system operation. MPC offers a promising alternative to reactive controllers which are the default in buildings today (Afram and Janabi-Sharifi, 2014). MPCs use a prediction model to estimate future states in buildings based on current conditions and forecasted disturbances (e.g. occupancy, solar gains). Optimal control inputs are then determined by minimizing a predefined cost function over a certain prediction horizon. MPCs routinely outperform other controller types in maintaining thermal comfort while minimizing energy consumption and/or cost, with energy savings of 9%-50% commonly reported in MPC studies (Afram and Janabi-Sharifi, 2014; Feng et al., 2015; Joe and Karava, 2019; Rockett and Hathway, 2017; Schwenzer et al., 2021).

Energy savings can also be achieved with energy-efficient conditioning systems, like radiant floors which can provide improved thermal comfort at lower energy costs (Fabrizio et al., 2012; Higgins and Carbonnier, 2017). However, controlling these systems can be challenging for reactive controllers because of their slow response times (Feng et al., 2015; Joe and Karava, 2019). Joe and Karava (2019) conducted a study comparing a MPC to a reactive controller in simulation, and in a real office building with radiant floor heating and cooling. The MPC reduced cooling energy consumption by 14% in simulation, and 16% in implementation, and reduced heating energy consumption by 20% in simulation, and 16% in implementation. Further energy savings can be realized with larger glazing areas to offset heating demands, but this may lead to overheating, even during the heating season (O'Brien et al., 2011; Ulpiani, 2017). Ulpiani (2017) showed, in an implementation study, that MPCs outperform other controller types in maintaining comfortable temperatures in such buildings.

Despite its growing popularity, MPC studies are largely simulation-based, with little attention paid to residential buildings. Schwenzer et al. (2021) found that only 4% of MPC studies related to indoor climate control included residential buildings. This gap in the literature is attributed to the lack of data collection infrastructure (required for prediction model development), a lack of building automation systems, and lower thermal inertia which makes residential buildings sensitive to disturbances (Wang et al., 2023). However, the first two of these limitations are mitigated by the increasing prevalence of smart thermostats in residential buildings

(Vallianos et al., 2023). Additionally, when MPCs are implemented in real buildings or laboratory environments, these studies often span just a few days (Rockett and Hathway, 2017). The lack of implementation studies is attributed to the large amount of effort required to implement MPCs, and the risk of discomfort in occupied buildings (Schwenzer et al., 2021). CHEeR therefore presents a perfect testing ground for MPC.

CHEeR is a full-scale, unoccupied research facility on Carleton University's campus in Ottawa, Canada. The facility mimics a single detached house, typical of Canadian households, with a large glazed area on the south facade (30% of the south wall area), and moderate-to-no glazing on the north, east, and west facades. CHEeR is equipped with several thermal capture and storage systems, as well as hydronic floor heating and cooling (Brown and Beausoleil-Morrison, 2021). Brideau et al. (2020) conducted simulations exploring the performance of different controller types in maintaining thermal comfort in a model based on CHEeR, investigating four floor constructions, and two glazing areas. The MPC was beneficial in high-glazing scenarios, where it had improved thermal comfort and/or energy use for all floor constructions. The MPC's peak operative temperature was at least 0.5°C lower, and time spent outside the comfortable temperature range was reduced by at least 40 minutes compared to other controllers. Additionally, Brown and Beausoleil-Morrison (2023) conducted an implementation study of a MPC at CHEeR spanning 182 days during the heating season. 71% of the experimental period had no significant overheating, or excessive use of cooling. Initial simulation studies also showed a 28% reduction in active cooling hours, and a 27% reduction in active heating hours compared to a reactive controller. These compelling results motivated the current work which makes improvements on the previous MPC formulation to maintain comfortable temperatures while minimizing energy consumption. The improvements include a novel prediction model structure with time-invariant parameters and time-variant disturbances, and a novel parameter estimation technique and weather forecasting approach.

Methodology

MPC development can be described in three phases. In phase one, parameters in an inverse model are estimated based on experimental data collected by Brown and Beausoleil-Morrison (2023). In phase 2, a forecasting procedure is used to estimate disturbances. In phase 3, control sequences are chosen based on a cost function and optimization algorithm.

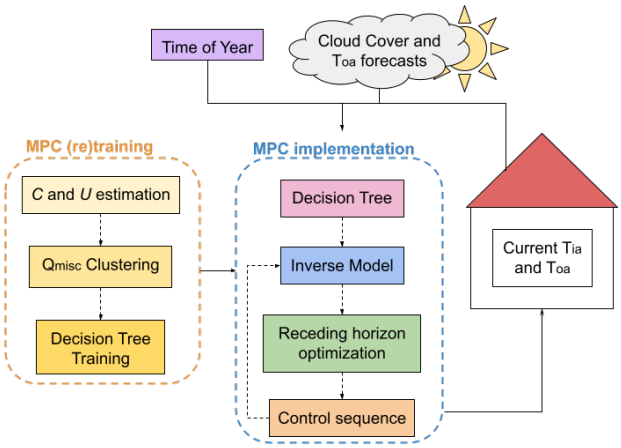

Figure 1: Flow chart showing implementation process of MPC

Inverse model

A single-node thermal resistance-capacitance model is formulated as shown below:

$$C\frac{dT_{ia}}{dt} = U(T_{oa} - T_{ia}) + Q_{hvac} + Q_{misc} \qquad (1)$$

where C (kJ/°C) and U (kW/°C) are the thermal capacitance and the thermal transmittance respectively, T_{ia} is the indoor air temperature, T_{oa} is the outdoor ambient air temperature, Q_{hvac} (kW) is the heat addition or extraction rate from the hydronic floors, and Q_{misc} (kW) represents heat gains from other sources (equipment, lighting, passive solar gains etc). A simple model was preferred to limit modeling effort, and maintain feasibility. Single-node models have been used successfully in other studies for whole-building control purposes (Date et al., 2016; Candanedo et al., 2022).

Parameter estimation

C was estimated using an approach developed by Gunay et al. (2023) to characterize thermal zones for fault-impact analysis. An overview is given here for completeness. First, data collected by Brown and Beausoleil-Morrison (2023) was filtered based on the following criteria:

- Data was gathered at night (to eliminate the effect of solar gains)
- Hydronic floors were off for three hours or more and then on for at least one hour (so enough time has passed that steady-state conditions can be assumed)

Filtering the data allows the prediction model to be further simplified. Since the focus is on conditions immediately before and after the hydronic floors became operational, Q_{misc}, and the envelope loss term are as-

sumed to be approximately constant and therefore cancel out in the following simplification that facilitates a straightforward solution for C:

$$C\frac{dT_{ia}}{dt}\bigg|_{t+1} - C\frac{dT_{ia}}{dt}\bigg|_{t-1} = Q_{hvac,t+1} - Q_{hvac,t-1}$$

$$C = \frac{Q_{hvac,t+1} - Q_{hvac,t-1}}{\frac{dT_{ia}}{dt}|_{t+1} - \frac{dT_{ia}}{dt}|_{t-1}} \quad (2)$$

where the Q_{hvac} and $\frac{dT_{ia}}{dt}$ terms are averaged over the hour preceding $(t-1)$ and following $(t+1)$ when the hydronic floors became operational. Equation 2 was used to estimate C values for all instances meeting the conditions described above, and a final C value was determined by taking their median.

The U coefficient was determined using linear regression analysis. The data was once again filtered based on the criteria described previously, plus the condition that the outdoor temperatures were less than 0°C to ensure envelope losses were sufficient. This filtering scheme allows a simplification of equation 1 since Q_{hvac} can be neglected, and Q_{misc} can be assumed to be constant since solar gains are excluded. The regression equation is given by the formula below:

$$C\frac{dT_{ia}}{dt} = U(T_{oa} - T_{ia}) + Q_{misc} \quad (3)$$

The filtered data and the previously determined C value were then used with equation 3 to estimate U.

Q_{misc} values were easily determined using equation 1, and were then used to develop a forecasting procedure, described in the following section. Q_{hvac} was determined explicitly for the estimation of C and Q_{misc} using the formula below:

$$Q_{hvac} = c_w \cdot q_{flow} \cdot (T_{sup} - T_{ret}) \quad (4)$$

where c_w is the heat capacity of water ($4.184\frac{\text{kJ}}{\text{kg°C}}$), q_{flow} is the mass flow rate of water (kg/s), and T_{sup} and T_{ret} are the supply and return temperatures of the hydronic floors. However, during implementation, when exact flow rates, and return and supply temperatures are unknown, average heat addition and extraction rates of 7kW and -7kW were used as rough estimates for Q_{hvac} based on data gathered by Brown and Beausoleil-Morrison (2023). Therefore equation 4 was used exclusively for parameter estimation.

Disturbance forecasting

To enable accurate indoor temperature predictions, Q_{misc} values (which are dominated by solar gains for highly glazed buildings) at different times of day and under different weather conditions need to be estimated. So, a procedure was developed to predict Q_{misc} based on the time of year, and forecasted cloud cover. This procedure is inspired by the work of Ashouri et al. (2018) and Hobson et al. (2020). In the current work, a K-means clustering algorithm is used to group days based on their hourly Q_{misc} values. This resulted in three distinct groups that can be broadly classified as "cloudy", "partly cloudy", and "clear" days. The average hourly values from these groups were then used to create a typical daily Q_{misc} profile for each day type, illustrated in Figure 2. These Q_{misc} profiles are then used as inputs to the prediction model. Negative values of Q_{misc} may indicate heat losses to the ground through basement walls, or to water storage tanks.

To predict which day type, and therefore which Q_{misc} profile to expect, a decision tree was used for rule extraction based on the daily average cloud cover between 7 am and 3 pm, and a parameter describing the time of year. The time of year was given by the month in a cyclical format based on the Sun's trajectory at different times of year. For example, December was given a value of 0 (lowest solar elevation), and June was given a value of 6 (highest solar elevation), meanwhile, March and September are given values of 3 (medium solar elevation). This parameter is referred to as the "cyclical month". The decision tree is illustrated in Figure 3.

Receding horizon optimization

The cost function took the following form:

```
if T_ia < 19.5:
    cost = S_htg + S_clg + 5 · (19.5 − T_ia)^2
else if T_ia > 25:
    cost = S_htg + S_clg + 5 · (T_ia − 25)^2
else:
    cost = S_htg + S_clg
```

Listing 1: Cost function

where S_{htg} and S_{clg} are boolean values indicating if heating and cooling are operational. These terms represent the "cost" associated with the operation of heating and cooling equipment to penalize excessive conditioning. The squared terms are the "cost" of deviations outside the comfortable range, where the power of two ensures that large deviations are penalized more severely. The comfortable range of 19.5°C to 25°C was chosen to match Brown and Beausoleil-Morrison (2023). This cost function is used with a genetic optimization algorithm to determine an optimal control sequence. This optimization algorithm is provided by Python's differential evolution function in the Scipy library. A population size of 70 and a maximum of 10 iterations were used after some trial and error to find a balance between run-time and solution quality.

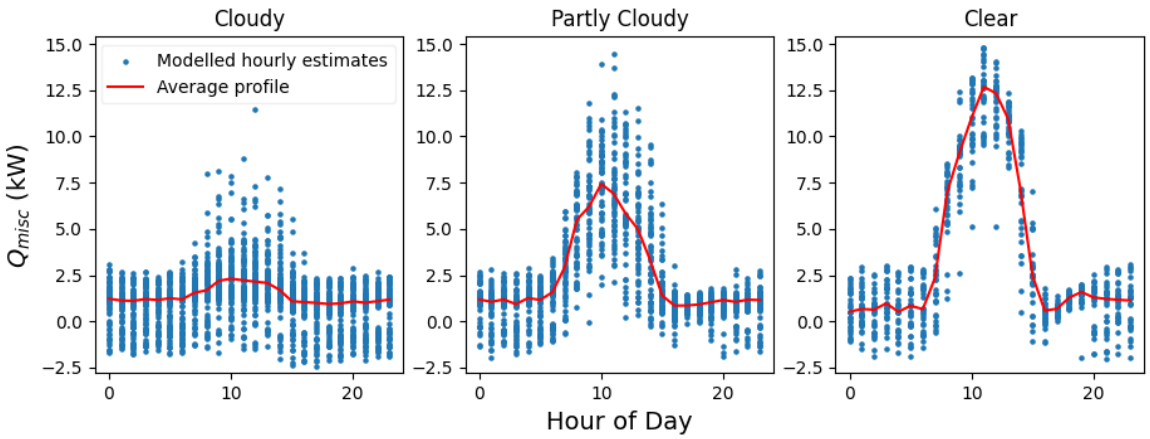

Figure 2: Derived Q_{misc} estimates and average daily profiles for each clustered day type: cloudy, partly cloudy, and clear

Case study implementation

The MPC is implemented at CHEeR during the heating season (November to early May), and controls the operation of the hydronic floors on both the first and second storey at CHEeR, treating them as one zone. An electric boiler and a water-to-water heat pump supply hot and cold water respectively. A receding horizon optimization process was used, with a prediction horizon of four hours, and a control timestep of 20 minutes. The prediction horizon aligns with that of Brown and Beausoleil-Morrison (2023), while the control timestep was shortened from 30 minutes as per the authors' recommendations.

Every 20 minutes, cloud cover forecasts and the cyclical month are sent to the decision tree which determines what Q_{misc} profile to expect. Current indoor temperatures at CHEeR along with outdoor temperatures forecasts, and the Q_{misc} values appropriate for the estimated day type and time of day are read into equation 1 to estimate future temperature profiles for many possible control sequences. These temperature profiles are sent to the cost function (Listing 1), and the optimization algorithm chooses the least costly control sequence. The first element of the control sequence is then implemented at CHEeR, effective for 20 minutes, and the process repeats. This procedure is represented visually in Figure 1.

For the first month of implementation, The MPC is trained on data gathered by Brown and Beausoleil-Morrison (2023). Following the first month, the MPC is re-trained bi-weekly using data gathered during the current experiment to account for changes in the facility that may impact heat transfer and storage processes, and to mimic real-life implementation where data may not be available to pre-train the model. A three-month moving window is kept as training data as the experiment progresses. Each time the model is re-trained, C, U, the Q_{misc} profiles, and the decision tree are updated.

For the first month of the implementation (November 8th to December 12th), due to a coding error, the control instructions were only implemented twice every hour at unequal intervals. Control decisions changed at the top of every hour and at the 20-minute mark, but the 40-minute mark was skipped over.

Baseline controller and performance metrics

To enable comparisons to another controller type, a RBC was used every other week in place of the MPC. This RBC activates cooling at 25°C and remains operational until CHEeR cools to 24.5°C. Heating is activated at 19.5°C and remains operational until CHEeR heats up to 20.5°C. The supply temperatures, and flow rates of the hydronic floors are the same as with the MPC.

To assess the performance of each controller, the amount of overheating was quantified using a metric described by Brown and Beausoleil-Morrison (2023). A summary is given here for completeness. The degree of overheating for a given day is quantified by both the magnitude and duration of deviations. The formula below was used to calculate "overheating performance" ($P_{overheat}$) in degree-hours.

$$P_{overheat} = \int (T_{ia} - T_{overheat}) H(T) dt \qquad (5)$$

where $T_{overheat}$ (°C) is the upper comfort threshold (25°C), and $H(T)$ is a Heaviside step function equal to 1 when $T_{ia} > T_{overheat}$ and 0 otherwise. Larger values of $P_{overheat}$ indicate higher degrees of overheating in magnitude and/or duration. Controller performance was also quantified by average daily energy use.

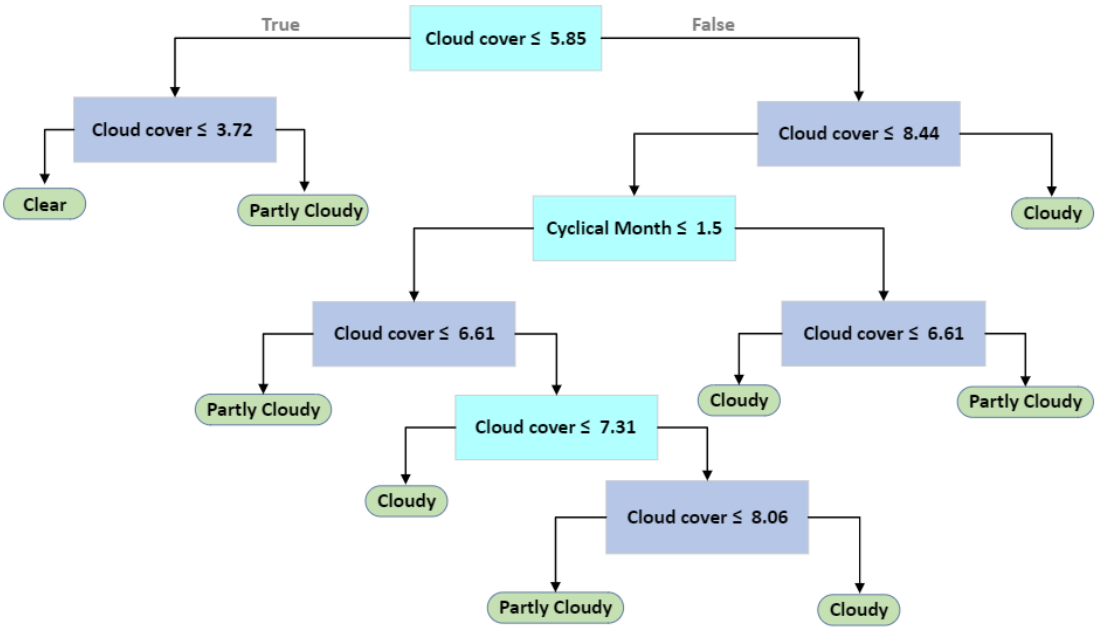

Figure 3: Decision tree used to estimate day types

Results and discussion

Overall Performance

For the first three months of the experimental period, the MPC achieved a 15% reduction in daily average energy use compared to the RBC. This was brought on by a 21% reduction in active heating hours, and a 46% reduction in active cooling hours. The weather under MPC and RBC operation differed slightly. The average heating degree days were 18.9°C, and 20.3°C for the MPC and RBC respectively. The average daily global horizontal irradiance (GHI) was 1.15$\frac{\text{kWh}}{\text{m}^2}$, and 1.23$\frac{\text{kWh}}{\text{m}^2}$ for the MPC and RBC respectively. A comparison of average daily energy use from different sources is provided in Figure 4. As well, on days that experienced some degree of overheating, the average overheating performance of the MPC was 0.544 degree-hours (equivalent to 0.544°C of overheating for one hour), contrasted with the RBC with an average overheating performance of 2.86 degree-hours. From Figure 5, the maximum temperatures reached by the MPC are generally lower than the RBC. However, the MPC occasionally allows temperatures to fall below the lower limit of 19.5°C, the cause of these deviations is detailed in the discussion of underheating on cloudy days below.

It is useful to assess MPC performance on individual days to identify strengths and weaknesses. A selection of well, and poorly-performing days are presented in the following sections along with comparisons between the MPC and RBC under different weather conditions.

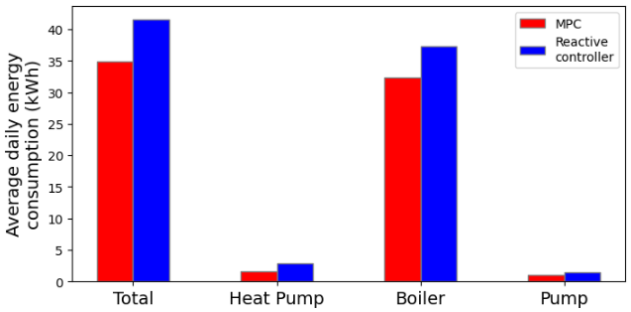

Figure 4: Average daily energy consumption from different sources under MPC and RBC operation

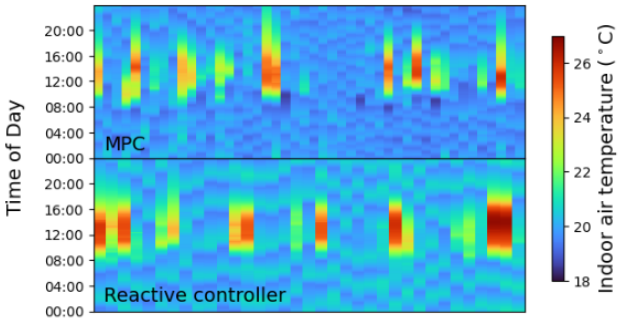

Figure 5: Heat map showing daily indoor temperature profiles for the first three months of the experimental period under MPC and RBC operation

Performance on sunny days: MPC versus RBC

November 20th (RBC) and 24th (MPC) were sunny days with very similar GHI profiles, requiring cooling to maintain thermal comfort. Figure 6 shows the in-

door and outdoor temperature profiles and active cooling periods for both the 20th and the 24th. On the 20th, the RBC did not activate cooling until CHEeR had reached 25°C just before 11:00. Because of the high magnitude of solar gains, CHEeR continued to heat up until around 13:00, reaching a peak temperature of 25.5°C. Meanwhile, the MPC correctly classified the 24th as "clear", activated cooling preemptively at 8:20, and deactivated cooling around when the temperature at CHEeR began to decrease naturally, reaching a much lower peak temperature of 24.1°C. The MPC had improved thermal comfort compared to the RBC, and achieved a 12.4% decrease in cooling energy use.

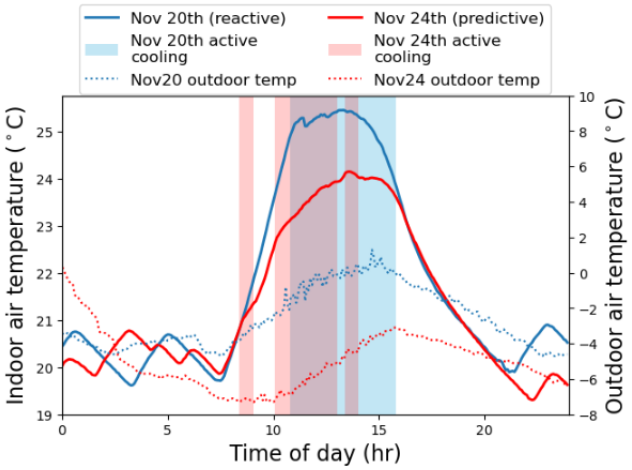

Figure 6: Indoor and outdoor air temperatures and active cooling times at CHEeR on November 20th (RBC operation) and November 24th (MPC operation)

Performance on cloudy days: MPC versus RBC

December 27th (RBC) and 28th (MPC) were both cloudy days with similar outdoor temperature and GHI profiles, and required heating throughout the day. Figure 7 shows the indoor and outdoor temperature profiles, along with active heating times for both days. While both controllers were able to maintain temperatures above 19.5°C for most of the day, the MPC reached a lower minimum temperature of 19.4°C. The MPC had a reduced number of active heating hours compared to the RBC, decreasing energy use by 4.8%.

Overcooling on partly cloudy days

November 11th was a partly cloudy day with cloud cover forecasts between four and eight tenths. At 11:00, the cloud cover forecasts dropped to four tenths although there was no noticeable change in the GHI readings at CHEeR during this time. As a result, the MPC changed the day's classification to "clear" and activated cooling unnecessarily, when the temperature at CHEeR was already decreasing naturally, resulting in 14 MJ of excessive cooling energy used.

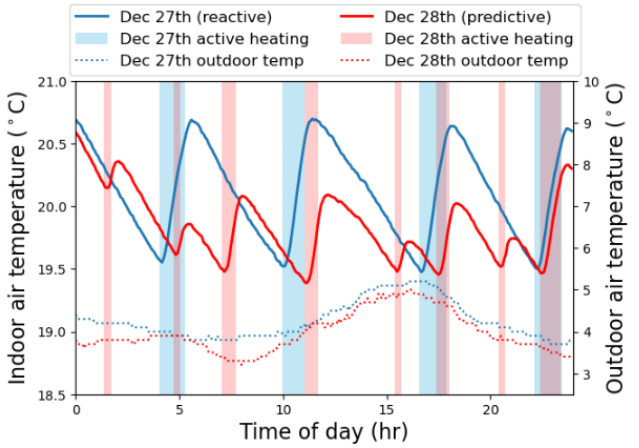

Figure 7: Indoor and outdoor air temperatures, and active heating times at CHEeR on December 27th (RBC operation) and December 28th (MPC operation)

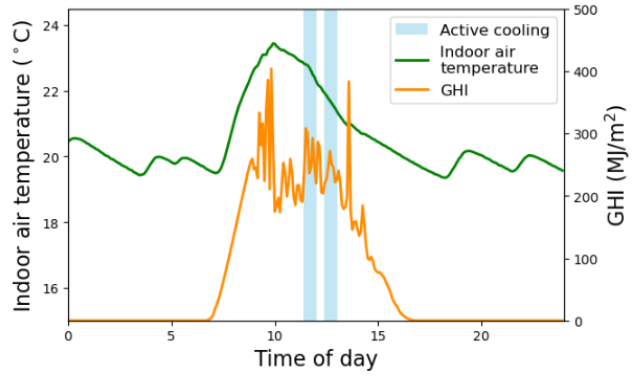

Figure 8: Indoor air temperature, GHI readings, and active cooling times at CHEeR on November 11th under MPC operation

Underheating on cloudy days

December 17th was a cloudy day, with cloud cover forecasts between eight and ten tenths. Despite the high cloud cover, the MPC classified the day as "clear" between 5:00 and 10:00. The MPC allowed indoor temperatures to fall below 19.5°C in anticipation of a high level of solar gains that never came, reaching a minimum temperature of 18.6°C before the MPC activated heating, and reclassified the day as "cloudy". This was the lowest indoor temperature seen under MPC operation. However, some less extreme deviations were caused by the same misclassification, where the MPC allowed some underheating in expectation of solar gains on cloudy days. Underheating is also caused by the discrete nature of control sequences. Since control inputs only change every 20 minutes, temperatures may drop slightly below 19.5°C before heating is activated.

Overheating on sunny days

February 8th was a sunny day, with cloud cover forecasts between one and four tenths. However, the MPC

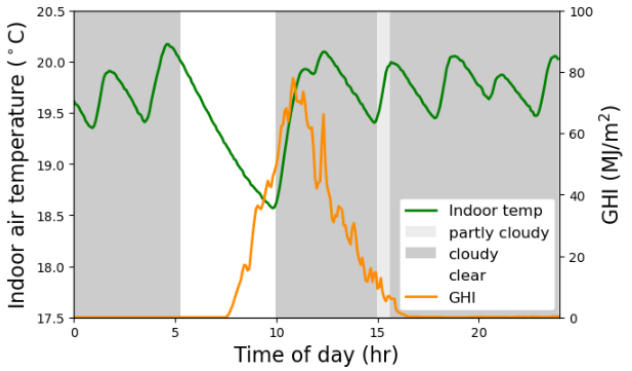

Figure 9: Indoor air temperatures, day type classifications, and GHI readings at CHEeR on December 17th under MPC operation

had chosen a "partly cloudy" classification for most of the day and therefore delayed cooling until CHEeR reached 25°C. As a result, the facility continued to heat up, reaching a maximum temperature of 26°C, with an overheating performance of 1.55 degree-hours. This was the most extreme overheating under MPC operation for the first three months of the experimental period.

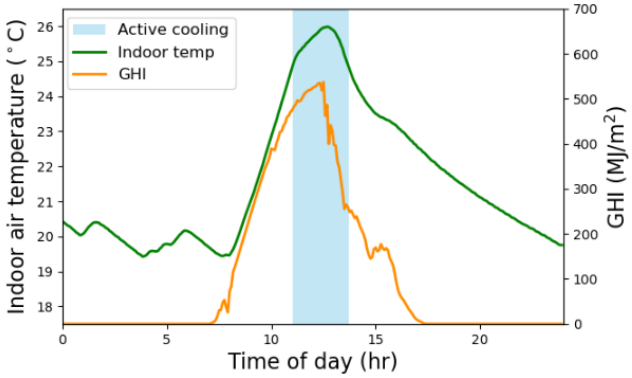

Figure 10: Indoor air temperature, active cooling times, and GHI at CHEeR on February 8th under MPC operation

Discussion

Although the MPC has shown improved thermal comfort and energy efficiency overall, November 11th, December 17th, and February 8th highlight some areas for improvement. First, the MPC is highly reliant on accurate cloud cover forecasts and day classifications since it does not use other weather indicators such as rates of change of the indoor air temperature at CHEeR. So, on days with inaccurate forecasts or questionable day classifications, the MPC cannot tell that this information may be faulty, leading to poor decisions. This could be alleviated in future work by including additional terms in the cost function to check that observed conditions at CHEeR match expectations. As well, the decision tree may require more training to produce accurate results.

During the first three months of the experimental period, it was noted that there were very few completely clear days. This lack of representation in the training data may explain the MPC's poor performance on February 8th. As well, on December 17th, the MPC's training dataset included less than six weeks of data, potentially contributing to the misclassification.

This MPC formulation procedure is easily duplicable in real buildings with the emergence of smart thermostats and building energy management systems (Vallianos et al., 2023). With proper data availability and training the MPC has the potential to improve thermal comfort and energy use in buildings with hydronic floor conditioning and high glazing. Future work could incorporate dynamic electricity pricing into the cost function to introduce additional benefits by minimizing energy costs on top of consumption.

Conclusion

A MPC development scheme was presented, detailing parameter estimation for a single-node thermal resistance-capacitance model, a disturbance forecasting procedure using clustering and rule extraction with a decision tree, and a receding horizon optimization algorithm. The MPC is trained on data from an experimental facility, CHEeR, at Carleton University, and subsequently implemented at CHEeR during the heating season. Results from the first three months of implementation are presented and compared to a RBC. The MPC achieved a 15% reduction in energy consumption due to a 21% and 46% decrease in active heating and cooling hours respectively. On sunny days the MPC can anticipate overheating and initiate cooling pre-emptively to avoid discomfort. Additionally, the MPC can anticipate when indoor temperatures will decrease naturally, avoiding unnecessary cooling. Some shortfalls include the MPC's reliance on accurate cloud cover forecasts, and the potential for the decision tree to classify days incorrectly. These factors have resulted in excessive cooling, overheating, and underheating. The MPC's performance could benefit from the inclusion of rates of change of indoor temperatures to "double-check" day-type classifications and forecasts. Additionally, incorporating dynamic electricity pricing could extend the benefits of the MPC by minimizing cost as well as consumption.

Acknowledgment

This work was supported by research funding provided by the Natural Sciences and Engineering Research Council of Canada. The authors also thank Sarah Brown and Tom Manser for their mentorship.

References

Afram, A. and F. Janabi-Sharifi (2014). Theory and applications of hvac control systems – a review of model predictive control (mpc). *Building and Environment 72*, 343–355.

Ashouri, A., Y. Hu, G. R. Newsham, and W. Shen (2018). Energy performance based anomaly detection in non-residential buildings using symbolic aggregate approximation. *IEEE*.

Brideau, S. A., I. Beausoleil-Morrison, and M. Kummert (2020). Effects of controls and floor construction of radiant floor heating systems for residential application with high variability of solar gains. *Science and Technology for the Built Environment 26*(4), 524–540.

Brown, S. and I. Beausoleil-Morrison (2021). Investigation of a model predictive controller for use in a highly glazed house with hydronic floor heating and cooling. *Science and Technology for the Built Environment 29*(4), 347–365.

Brown, S. and I. Beausoleil-Morrison (2023). Long-term implementation of a model predictive controller for a hydronic floor heating and cooling system in a highly glazed house in canada. *Applied Energy 349*, 121677.

Candanedo, J. A., C. Vallianos, B. Delcroix, J. Date, A. S. Derakhtenjani, N. Morovat, C. John, and A. K. Athienitis (2022). Control-oriented archetypes: a pathway for the systematic application of advanced controls in buildings. *Journal of Building Performance Simulation 15*(4), 433–444.

Date, J., J. A. Candanedo, and A. K. Athienitis (2016). Control-oriented modelling of thermal zones in a house: a multi-level approach. *International High Performance Buildings Conference*.

Fabrizio, E., S. Corgnati, F. Causone, and M. Filippi (2012, 08). Numerical comparison between energy and comfort performances of radiant heating and cooling systems vs. air systems. *HVACR RESEARCH 18(4)*, 692–708.

Feng, J. D., F. Chuang, F. Borrelli, and F. Bauman (2015). Model predictive control of radiant slab systems with evaporative cooling sources. *Energy and Buildings 87*, 199–210.

Gunay, B., B. W. Hobson, D. Darwazeh, and J. Bursill (2023). Estimating energy savings from hvac controls fault correction through inverse greybox model-based virtual metering. *Energy Buildings*.

New Buildings Institute (2017). *Energy Performance of Commercial Buildings with Radiant Heating and Cooling*.

Hobson, B. W., H. B. Gunay, and A. Ashouri (2020). Wi-fi based occupancy clustering and motif identification: A case study. *ASHRAE Transactions*.

Joe, J. and P. Karava (2019). A model predictive control strategy to optimize the performance of radiant floor heating and cooling systems in office buildings. *Applied Energy 245*, 65–77.

Natural Resources Canada (2019). Cooling and ventilation equipment for residential use. `https://natural-resources.canada.ca/energy-efficiency/products/cooling-and-ventilating-equipment-for-residential-use/13756` [Accessed: (2024-01-15)].

Natural Resources Canada (n.d.). Energy efficiency trends analysis tables: Total end-use sector-energy use analysis. `https://oee.rncan.gc.ca/corporate/statistics/neud/dpa/showTable.cfm?type=AN&sector=aaa&juris=ca&year=2020&rn=1&page=0` [Accessed: (2024-01-15)].

O'Brien, W., A. Athienitis, and T. Kesik (2011). Thermal zoning and interzonal airflow in the design and simulation of solar houses: a sensitivity analysis. *Journal of Building Performance Simulation 4*(3), 239–256.

Rockett, P. and E. A. Hathway (2017). Model-predictive control for non-domestic buildings: a critical review and prospects. *Building Research & Information 45*(5), 556–571.

Schwenzer, M., M. Ay, T. Bergs, and D. Abel (2021). Review on model predictive control: an engineering perspective. *The International Journal of Advanced Manufacturing Technology 117*, 1327 – 1349.

Ulpiani, G. (2017). Overheating phenomena induced by fully-glazed facades: Investigation of a sick building in italy and assessment of the benefits achieved via fuzzy control of the ac system. *Solar Energy 158*, 572–594.

Vallianos, C., J. Candanedo, and A. Athienitis (2023). Application of a large smart thermostat dataset for model calibration and model predictive control implementation in the residential sector. *Energy 278*, 127839.

Wang, D., Y. Chen, W. Wang, C. Gao, and Z. Wang (2023). Field test of model predictive control in residential buildings for utility cost savings. *Energy and Buildings 288*, 113026.